JOURNAL OF GEOPHYSICAL RESEARCH, VOL. 86, NO. A7, PAGES 5793–5800, JULY 1, 1981

Chemical Fluctuations and Incoherent Scattering Theory in the Terrestrial *D* Region

G. KOCKARTS AND J. WISEMBERG

Institut d'Aéronomie Spatiale, B-1180 Bruxelles, Belgium

The continuum theory of incoherently scattered electromagnetic waves is modified in order to include possible effects of thermally induced chemical fluctuations. These fluctuations are taken into account by introducing fluctuating parts in the production and loss terms of the continuity equations. An equivalent ionospheric model is developed for three types of ionized species, i.e., electrons and negative and positive ions. A matrix formulation gives simultaneous access to fluctuating parts of each charged component. Numerical results indicate that chemical fluctuations are important over the height range where negative ions are comparable or greater than the electron concentration. Strong enhancements of the incoherent scatter cross section occur for frequency shifts smaller than approximately 20 Hz. A simple approximation is given for the contribution of chemical fluctuations.

INTRODUCTION

Incoherent or Thomson scattering is a powerful tool for numerous investigations of the upper atmosphere [see *Evans,* 1969; *Bauer,* 1975; *Alcaydé,* 1979; *Walker,* 1979]. Recently, additional interest was given to the contribution of large radars to middle atmosphere studies between 10-km and 100-km altitude [see *Harper and Gordon,* 1980]. In particular, measurements by *Harper* [1978] indicate that an ion component of the incoherent scatter spectrum is observable below 80-km altitude, where negative ions progressively become dominant.

The continuum theory of *Tanenbaum* [1968] for a collision-dominated incoherent scatter spectrum has been modified by *Mathews* [1978] and by *Fukuyama and Kofman* [1980] to include the effects of negative ions. Hydrodynamic equations used by these authors are essentially identical to the equations adopted by *Tanenbaum* [1968]. The major difference comes from the introduction of a continuity, momentum, and energy equation for a negative ion, and following the arguments of *Dougherty and Farley* [1960], the spectrum is considered as a result of thermal fluctuations of the ambient electrons. Continuity equations are, however, written without production or loss terms.

When electron thermal fluctuations are present, it is conceivable that such fluctuations also induce fluctuations of the production and loss terms. In the present paper these terms are kept in the continuity equations for the three charged species, and a matrix formulation is developed to investigate which effect can produce results on the incoherent scatter cross section. Since production and loss terms depend on physical mechanisms influencing the lower *D* region, it is necessary to have a quantitative evaluation for the various production or loss rates which are proportional to charged particle concentrations. An equivalent ionospheric model is therefore constructed in section 2 by using the signal flow graph theory developed by *Wisemberg and Kockarts* [1980]. With such a model, a theoretical expression is deduced for the incoherent scatter cross section in section 3, and this expression reduces to the results of *Mathews* [1978] and *Fukuyama and Kofman* [1980] when chemical fluctuations are ignored. An application to the lower *D* region is presented in section 4, where it appears that the incoherent scatter cross section is strongly enhanced for low-frequency shifts in the height region below 75 km. Since the enhancement essentially depends on the ratio between negative ions and electrons, it can be concluded that mesospheric incoherent scatter observations provide an excellent tool for the determination of the negative ion abundance.

Paper number 1A0481.
0148-0227/81/001A-0481$01.00

2. EQUIVALENT IONOSPHERIC MODEL

More than 100 ion-neutral reactions involved in the construction of a detailed theoretical model of the terrestrial *D* region lead to several types of negative and positive ions. Incoherent scatter theory is, however, more tractable if only three types of charged particles are to be considered. It is therefore useful to reduce a multicomponent model to an equivalent model which consists of electrons e, positive ions X^+, and negative ions X^-. Such a reduction is rather easy when the detailed model is constructed by using a signal flow graph technique as described by *Wisemberg and Kockarts* [1980].

Five equivalent processes are sufficient to reproduce the total negative, positive, and electron concentrations if equivalent or effective reaction rates can be deduced from a multicomponent model in which the external production rate γ_e (cm^{-3} s^{-1}) for electrons and positive ions is given. These reactions can be schematized as follows:

$$\text{input} \rightarrow e + X^+;\ \gamma_e(\text{cm}^{-3}\ \text{s}^{-1}) \tag{1}$$

$$\text{neutrals} + e \rightarrow X^-;\ n_e L_e\ (\text{cm}^{-3}\ \text{s}^{-1}) \tag{2}$$

$$\text{neutrals or light} + X^- \rightarrow e;\ n_- L_-\ (\text{cm}^{-3}\ \text{s}^{-1}) \tag{3}$$

$$e + X^+ \rightarrow \text{neutrals};\ \alpha_e n_e n_+\ (\text{cm}^{-3}\ \text{s}^{-1}) \tag{4}$$

$$X^- + X^+ \rightarrow \text{neutrals};\ \alpha_- n_- n_+\ (\text{cm}^{-3}\ \text{s}^{-1}) \tag{5}$$

where the concentrations of positive ions X^+ and negative ions X^- are given by n_+ and n_-, respectively. The electron concentration n_e can be affected by attachment processes with an effective loss rate L_e (s^{-1}) and by electron-ion recombination with an effective rate α_e (cm^3 s^{-1}). Negative ions can be lost by collisional detachment, by photodissociation, and by photodetachment with an effective loss rate L_- (s^{-1}) or by ion-ion neutralization with an effective recombination rate α_- (cm^3 s^{-1}).

In presence of j different positive ions with concentrations n_j^+ and i different negative ions with concentration n_i^-, an equivalent model is obtained if effective rate coefficients L_e, L_-, α_e, and α_- are available such that $n_+ = \sum_j n_j^+$ and $n_- =$

TABLE 1. Effective Rate Coefficients for the Equivalent Model

z, km	γ_e, cm^{-3} s^{-1}	L_e, s^{-1}	L_-, s^{-1}	α_e, cm^3 s^{-1}
50	3.20(−1)*	4.65(+1)	2.89(−3)	3.00(−6)
55	1.73(−1)	1.38(+1)	5.79(−3)	3.00(−6)
60	9.94(−2)	3.98(0)	2.13(−2)	3.00(−6)
65	6.19(−2)	1.08(0)	8.11(−2)	2.99(−6)
70	3.23(−1)	2.71(−1)	4.78(−1)	2.95(−6)
75	3.11(0)	5.24(−2)	2.23(0)	2.34(−6)
80	1.11(1)	1.16(−2)	4.99(0)	7.34(−7)

*For 3.20(−1), read 3.20×10^{-1}.

$\sum_i n_i^-$ with $n_+ = n_e + n_-$. The effective electron-ion recombination and ion-ion neutralization rates are given respectively by

$$\alpha_e = \left(\sum_j \alpha_j n_j^+ \right) \Big/ \sum_j n_j^+ \tag{6}$$

and

$$\alpha_- = \left(\sum_i n_i^- \sum_j \alpha_{ij} n_j^+ \right) \Big/ \left(\sum_i n_i^- \sum_j n_j^+ \right) \tag{7}$$

where α_j is the electron-ion recombination rate of the j-type positive ion and α_{ij} is the ion-ion neutralization rate between the i-type negative ion and the j-type positive ion. Numerical values for L_e and L_- cannot be found in such a simple manner, since one has to take into account the various loops leading from electrons to negative ions and vice and versa. Nevertheless, these quantities can be deduced from signal flow graph theory. *Wisemberg and Kockarts* [1980] have shown that the net electron production rate P_e resulting from an external input production γ_e associated with numerous chemical processes is given by

$$P_e = \gamma_e T_{(e \leftarrow IN)} \tag{8}$$

where $T_{(e \leftarrow IN)}$ represents the transmittance from the external input to the steady state electrons. When the net electron production rate (8) is equated to the total production rate resulting from processes (1) and (3), the effective loss rate L_- for negative ions can be written

$$L_- = \gamma_e (T_{(e \leftarrow IN)} - 1)/(\lambda n_e) \tag{9}$$

where $\lambda = n_-/n_e$. The net electron production rate (8) is also equal to the total electron loss rate resulting from processes (2) and (4). The effective electron loss rate L_e is therefore given by

$$L_e = \gamma_e T_{(e \leftarrow IN)}/n_e - \alpha_e n^+ \tag{10}$$

or

$$L_e = \lambda L_- + (\gamma_e/n_e) - \alpha_e n^+ \tag{11}$$

when the transmittance in (10) is replaced by its expression resulting from (9). All transmittances were computed in the model of *Wisemberg and Kockarts* [1980] and particularly $T_{(e \leftarrow IN)}$. Using (6), (7), (9), and (11), one obtains the numerical values for L_e, L_-, and α_e given in Table 1, which also provides the external input γ_e at 5-km height intervals in the lower ionosphere. The average ion-ion neutralization rate α_- is not given in Table 1, since all α_{ij} ion-ion neutralization rates were taken equal to 6×10^{-8} cm^3 s^{-1} in the Wisemberg and Kockarts model, leading therefore to a height-independent value $\alpha_- = 6 \times 10^{-8}$ cm^3 s^{-1}. Table 2 gives the neutral temperature T_n, the electron concentration n_e, the ratio $\lambda = n_-/n_e$, and the mean molecular masses m_+ and m_- for positive and negative ions, respectively. The last two quantities are given since they are necessary for computing incoherent scatter cross sections. All values in Tables 1 and 2 have been computed directly from the detailed ionospheric model. With the data of Table 1 it is, however, possible to compute independently the electron concentrations and λ values of Table 2. When all effective rates are known, it is easily shown that processes (1) to (5) lead to steady state electron concentration given by

$$n_e^2 = \gamma_e/[(1 + \lambda)(\alpha_e + \lambda\alpha_-)] \tag{12}$$

The ratio λ between negative ions and electrons is obtained from (11) under the form

$$\lambda = \frac{L_e}{L_-} \left[1 + \frac{n_e(1 + \lambda)\alpha_e}{L_-} \right]^{-1} \tag{13}$$

This expression is identical to equation (18.12) of *Banks and Kockarts* [1973], which can be written with present notation

$$\lambda = \frac{L_e}{L_-} \left[1 + \frac{\gamma_e}{(1 + \lambda)L_- n_e} + \frac{(\alpha_- - \alpha_e)n_e}{L_-} \right]^{-1} \tag{14}$$

When numerical values are introduced in (13) or (14), it appears that an excellent approximation of λ is given by

$$\lambda = L_e/L_- = n_-/n_e \tag{15}$$

Such an expression indicates that the ratio λ is mainly controlled by electron attachment and detachment processes and that recombination processes play a negligible role. This property will be used in the numerical computation of the incoherent scatter cross section which is derived in the following section.

3. Conservation Equations and Incoherent Scatter Cross Section

According to *Dougherty and Farley* [1960] the average differential scattering cross section for backscattering can be written as

$$\sigma(\omega_0 \pm \omega)d\omega = r_e^2 L^3 n_e' n_e'^* \, d\omega \tag{16}$$

where σ is the average power scattered through 180° per unit solid angle, per unit incident power, per unit volume, and per unit frequency range. The angular frequency of the incident wave is ω_0, the Doppler shift is ω, and $r_e = 2.82 \times 10^{-13}$ cm is the classical electron radius. Scattering is assumed to occur in a volume L^3 as a consequence of electron density fluctuations whose ensemble average is given by $n_e' n_e'^*$, $n_e'^*$ being the complex conjugate of n_e'. This ensemble average is a function of the Doppler shift ω and of a wave number k which is twice the incident wave number, in the case of backscattering.

Electron density fluctuations in the lower ionosphere can be

TABLE 2. Parameters of the Equivalent Model [*Wisemberg and Kockarts*, 1980]

z, km	T_n, K	n_e, cm^{-3}	$\lambda = n_-/n_e$	m_+, amu	m_-, amu
50	271	1.50(−1)*	1.53(4)	55	61
55	261	7.20(−1)	2.34(3)	55	61
60	247	6.11(0)	1.86(2)	54	61
65	233	3.39(1)	1.34(1)	53	61
70	220	2.64(2)	5.67(−1)	48	61
75	208	1.14(3)	2.35(−2)	42	55
80	198	3.86(3)	2.32(−3)	32	39

*For 1.50(−1), read 1.50×10^{-1}.

deduced from conservation equations [*Tanenbaum,* 1968; *Seasholtz and Tanenbaum,* 1969; *Seasholtz,* 1971; *Mathews,* 1978; *Fukuyama and Kofman,* 1980]. All previous computations implicitly assume that electron thermal fluctuations have no effect on the production and loss terms in the continuity equation. However, the effective electron lifetime becomes shorter in presence of negative ions, as can be seen from the effective loss terms given in Table 1. At 50-km altitude the electron effective lifetime is of the order of 2×10^{-2} s, whereas it reaches a value of the order of 100 s at 80-km altitude. In order to investigate the effect of thermally induced chemical fluctuations, we start from the 13-moment approximation of the conservation equation [*Schunk,* 1975, 1977]. When charged particles essentially exchange energy with the ambient neutral components and when magnetic field effects and Joule heating are negligible, the continuity momentum and energy equations can be written for each s-type ionized component as follows:

$$\frac{\partial n_s}{\partial t} + \nabla \cdot (n_s \mathbf{u}_s) = P_s - n_s L_s \tag{17}$$

$$\frac{\partial \mathbf{u}_s}{\partial t} + \mathbf{u}_s \cdot \nabla \mathbf{u}_s + \frac{1}{n_s m_s} \nabla p_s - \frac{\mathbf{F}_s}{m_s} - \frac{q_s}{m_s} \mathbf{E} - \frac{\eta_{sn}}{n_s m_s} [\nabla^2 \mathbf{u}_s + \tfrac{1}{3} \nabla (\nabla \cdot \mathbf{u}_s)] = -\nu_{sn} (\mathbf{u}_s - \mathbf{u}_n) \tag{18}$$

$$\frac{3}{2} \frac{\partial p_s}{\partial t} + \tfrac{3}{2} \mathbf{u}_s \cdot \nabla p_s + \tfrac{5}{2} p_s \nabla \cdot \mathbf{u}_s - \nabla (\lambda_{sn} \nabla T_s) = -\frac{3 n_s m_s \nu_{sn}}{m_s + m_n} K (T_s - T_n) \tag{19}$$

where n_s is the s-type particle concentration, $\mathbf{u}_s$ is its drift velocity, and P_s and L_s are the production and loss rates, respectively. In the momentum equation, $p_s = n_s K T_s$ is the scalar pressure of the s-type particle with temperature T_s, mass m_s, and electrical charge $q_s \cdot \mathbf{F}_s$ is any external force acting on the s-type particle, $\mathbf{E}$ is the electric field, η_{sn} is the viscosity coefficient of species s in the neutral gas n with drift velocity $\mathbf{u}_n$, temperature T_n, and mean molecular mass m_n. The thermal conductivity λ_{sn} refers to interactions between charged particles and the ambient neutral gas, and ν_{sn} is the electron or ion-neutral momentum transfer collision frequency. We follow the technique of *Tanenbaum* [1968] by assuming that the concentrations n_s, pressures p_s, and temperatures T_s are composed of static components (n_{s0}, p_{s0}, T_{s0}) and small fluctuating components (n_s', p_s', T_s') proportional to $e^{i(\omega t - kz)}$. The conservation equations are only considered along the vertical direction z, and the neutral gas is assumed at rest ($\mathbf{u}_n = 0$) as well as the static components u_{s0} for the charged particles. In addition, the vertical components F_s', E, and u_s' for the external forces, for the electric field, and for the charged particle velocities are all proportional to $e^{i(\omega t - kz)}$. With these assumptions it is possible to linearize the conservation equations (17) to (19).

When the production and loss rates resulting from processes (1) to (5) are introduced in the continuity equation (17), one obtains the following matrix relation between the fluctuating concentrations n_s' and drift speeds u_s':

$$\mathbf{A} \begin{bmatrix} n_e'/n_{e0} \\ n_-'/n_{-0} \\ n_+'/n_{+0} \end{bmatrix} = \frac{k}{\omega} \begin{bmatrix} u_e' \\ u_-' \\ u_+' \end{bmatrix} \tag{20}$$

when three types of charged particles are considered, i.e., $s = e$ for electrons, $s = -$ for negative ions, and $s = +$ for positive ions. The matrix $\mathbf{A}$ given by (A5) in the appendix depends on the effective loss rates L_e and L_- defined for the equivalent ionospheric model in section 2. It should be noted that without production and loss terms in the continuity equations, matrix $\mathbf{A}$ reduces to a unitary matrix. In such a case, all following results can be easily transformed to obtain the formulation developed by *Mathews* [1978] and by *Fukuyama and Kofman* [1980].

The linearization of the three energy equations (19) leads to

$$\begin{bmatrix} p_e'/n_{e0} \\ p_-'/n_{-0} \\ p_+'/n_{+0} \end{bmatrix} = ik\mathbf{Q} \begin{bmatrix} u_e' \\ u_-' \\ u_+' \end{bmatrix} + \mathbf{R} \begin{bmatrix} n_e'/n_{e0} \\ n_-'/n_{-0} \\ n_+'/n_{+0} \end{bmatrix} \tag{21}$$

where $\mathbf{Q}$ and $\mathbf{R}$ are diagonal matrices whose elements are given by (A6) and (A7) in the appendix.

Finally, it is shown in the appendix that the linearization of the three momentum equations (18) combined with expression (21) leads to

$$\mathbf{C} \begin{bmatrix} u_e' \\ u_-' \\ u_+' \end{bmatrix} + \frac{\omega}{k} \mathbf{D} \begin{bmatrix} n_e'/n_{e0} \\ n_-'/n_{-0} \\ n_+'/n_{+0} \end{bmatrix} = \frac{i\omega}{k^2 K T_e} \mathbf{T} \begin{bmatrix} F_e' \\ F_-' \\ F_+' \end{bmatrix} \tag{22}$$

where matrices $\mathbf{C}$, $\mathbf{D}$, and $\mathbf{T}$ are given in the appendix by (A15), (A14), and (A11), respectively. Combining (22) with the continuity equation (20), it is possible to express the concentration fluctuations by

$$\begin{bmatrix} n_e' \\ n_-' \\ n_+' \end{bmatrix} = \frac{i}{kKT_e} \mathbf{X} (\mathbf{CA} + \mathbf{D})^{-1} \mathbf{T} \begin{bmatrix} F_e' \\ F_-' \\ F_+' \end{bmatrix} \tag{23}$$

where $\mathbf{X}$ is a diagonal matrix with real elements n_{e0}, n_{-0}, and n_{+0}, respectively.

Since the incoherent scattering cross section is proportional to the ensemble average of the electron fluctuations, we define a concentration fluctuation matrix $\mathbf{N}$ by

$$\mathbf{N} = \begin{bmatrix} n_e' \\ n_-' \\ n_+' \end{bmatrix} [n_e'^* n_-'^* n_+'^*] \tag{24}$$

where $n_e'^*$, $n_-'^*$, and $n_+'^*$ are complex conjugate quantities. Using relation (23) between concentration fluctuations n_s' and perturbing forces F_s', (24) leads to

$$\mathbf{N} = (kKT_e)^{-2} \mathbf{H} \mathbf{F} \mathbf{H}^+ \tag{25}$$

where the force matrix $\mathbf{F}$ is defined in a similar way as $\mathbf{N}$ and $\mathbf{H}^+$ is the Hermitian conjugate matrix of $\mathbf{H}$ given by

$$\mathbf{H} = \mathbf{X} (\mathbf{CA} + \mathbf{D})^{-1} \mathbf{T} \tag{26}$$

By analogy with a theory developed by *Barakat* [1963] for optical instruments, $\mathbf{F}$ can be considered as an input coherency matrix leading to an output coherency matrix by the action of a transfer function matrix $\mathbf{H}$. The ensemble average value $n_e' n_e'^*$ required in (16) for the differential cross section is simply the first element of matrix $\mathbf{N}$.

Computation of the elements of matrix N requires an analytical expression for F which can be obtained from the fluctuation-dissipation theorem [see *Seasholtz,* 1971] relating the applied force matrix F to an impedance matrix Z by the relation

$$\mathbf{F} = \frac{KT_e}{2\pi L^3}(\mathbf{Z} + \mathbf{Z}^+) \tag{27}$$

where the impedance matrix Z is by definition such that

$$\begin{bmatrix} F_e' \\ F_-' \\ F_+' \end{bmatrix} = \mathbf{Z} \begin{bmatrix} \Gamma_e \\ \Gamma_- \\ \Gamma_+ \end{bmatrix} \tag{28}$$

$\Gamma_s = n_{s0}u_s'$ is the resulting flux density fluctuation for the s-type species. Comparing (28) with (23) and using the continuity equation (20), one obtains

$$\mathbf{Z} = k^2 KT_e \mathbf{W} \tag{29}$$

with

$$\mathbf{W} = (i\omega)^{-1}\mathbf{T}^{-1}(\mathbf{C} + \mathbf{D}\mathbf{A}^{-1})\mathbf{X}^{-1} \tag{30}$$

where all matrices in W have been previously defined. Combining (25), (27), and (30), the concentration fluctuation matrix can be written

$$\mathbf{N} = (2\pi)^{-1}L^{-3}\mathbf{H}(\mathbf{W} + \mathbf{W}^+)\mathbf{H}^+ \tag{31}$$

where $\mathbf{W}^+$ and $\mathbf{H}^+$ are Hermitian conjugates of W and H, respectively. The first diagonal term of N is the ensemble average $n_e'n_e'^*$ required in the differential scattering cross section given by (16) in which the volume term L^3 will be eliminated by the L^{-3} factor in (31). When $N_{(e,e)}$ is the first diagonal element of N computed without the L^{-3} factor, the differential backscattering cross section (16) is given by

$$\sigma(\omega_0 \pm \omega)\, d\omega = r_e^2 N_{(e,e)}\, d\omega \tag{32}$$

The other diagonal elements of N represent ensemble average fluctuations of negative and positive ions, respectively. Nondiagonal terms give cross-spectral density fluctuations. The matrix formulation previously developed provides a simultaneous access to these quantities.

4. Application to the Terrestrial *D* Region

The present formulation takes into account chemical fluctuations which are thermally induced on the production and loss terms in the continuity equation. When this equation is written without these terms, matrix A given by (A4) or (A5) reduces to a unitary matrix, and the differential backscattering cross section (32) becomes identical to the expression given by *Mathews* [1978] or by *Fukuyama and Kofman* [1980]. Although our mathematical formalism is different, it is not necessary to repeat here a discussion of the influence of negative ions on mesospheric incoherent scatter spectra in absence of chemical fluctuations.

The general backscattering cross section (32) requires a knowledge of effective loss rates involved in matrix A, concentrations of ionized species, temperatures, neutral and ionized mean molecular masses, neutral concentrations, and collision frequencies. The characteristics for the ionized components are given in Tables 1 and 2. Temperatures of the ionized species are assumed equal to the neutral temperature. The total neutral concentration and mean molecular mass are taken from the U.S. Standard Atmosphere (1976), and the electron-neutral and ion-neutral collision frequencies are computed with the expressions of *Banks and Kockarts* [1973]. All computations are made for an incident frequency $f_0 = 935$ MHz, which corresponds to the incoherent scatter station at Saint-Santin (44.6°N, 2.2°E).

Figure 1 shows the incoherent scatter cross section computed at 60-km, 70-km, and 80-km altitude as a function of the frequency shift $f_0 \pm f$. Solid curves refer to the left-hand ordinate, which corresponds to a normalized cross section. Dashed curves refer to the right-hand ordinate, which corresponds to real cross sections expressed in terms of the classical electron radius. The factors 2π are introduced by the relation $\omega = 2\pi f$ between angular and linear frequencies. These cross sections have the usual characteristics, with an ionic and an electronic component separated by a plateau. At low-frequency shifts, normalized cross sections are, however, larger at 60-km and 70-km altitude than at 80 km, where the electron concentration is nevertheless higher. Such an apparently anomalous phenomenon does not appear for the real cross section (dashed curves). Whereas the cross section is almost independent of frequency shifts below 30 Hz at 80-km altitude, a sharp increase still occurs at 60-km and 70-km altitude. Table 2 indicates that negative ions become important below 70-km altitude, where the effective loss rates L_e and L_- begin to play a significant role in the introduction of chemical fluctuations.

The practical importance of thermally induced chemical fluctuations is shown in Figure 2. Total cross sections computed from the full equation (32) are indicated by solid lines, and cross sections obtained with the theory of *Mathews* [1978] and *Fukuyama and Kofman* [1980] are represented by dashed lines. Values are again given for 60-km, 70-km, and 80-km altitude, but frequency shifts are limited to ±50 Hz in order to give a clear picture of the central portion of the spectrum including zero-frequency shift. The contribution of chemical fluctuations is negligible at 80 km, but at altitudes where λ becomes comparable or greater than 1, extremely large differences are obtained between σ_{total} and σ_{MFK}. This is particularly true for small frequency shifts. Depending on the values for λ and n_e, the present ionic spectrum always converges at some frequency shift toward the spectrum of *Mathews* [1978] and *Fukuyama and Kofman* [1980]. Chemical fluctuations only enhance incoherent scatter cross sections at small frequency shifts. Interpretation of observed incoherent scatter spectra below 80-km altitude in terms of chemical fluctuations requires a frequency resolution of the order of 1 Hz to 2 Hz in order to identify sharp peaks such as those computed here around 70-km altitude. Narrow spectra have been observed in the mesosphere at Arecibo [*Harper,* 1978; *Ganguly,* 1980]. Values for the parameter λ have been deduced by *Ganguly et al.* [1979], but it is not obvious from published spectra that frequency resolution was sufficient to extract an effect related to chemical fluctuations.

Interpretation of experimental spectra is easier when a simple analytical formula is available for the incoherent scatter cross section. Using the cross section σ_{MFK} given by *Mathews* [1978] and *Fukuyama and Kofman* [1980], we approximate the present cross section σ_T by

$$\sigma_T = \sigma_C + \sigma_{\text{MFK}} \tag{33}$$

where σ_C represents the contribution resulting from chemical fluctuations. It turns out that an excellent approximation for

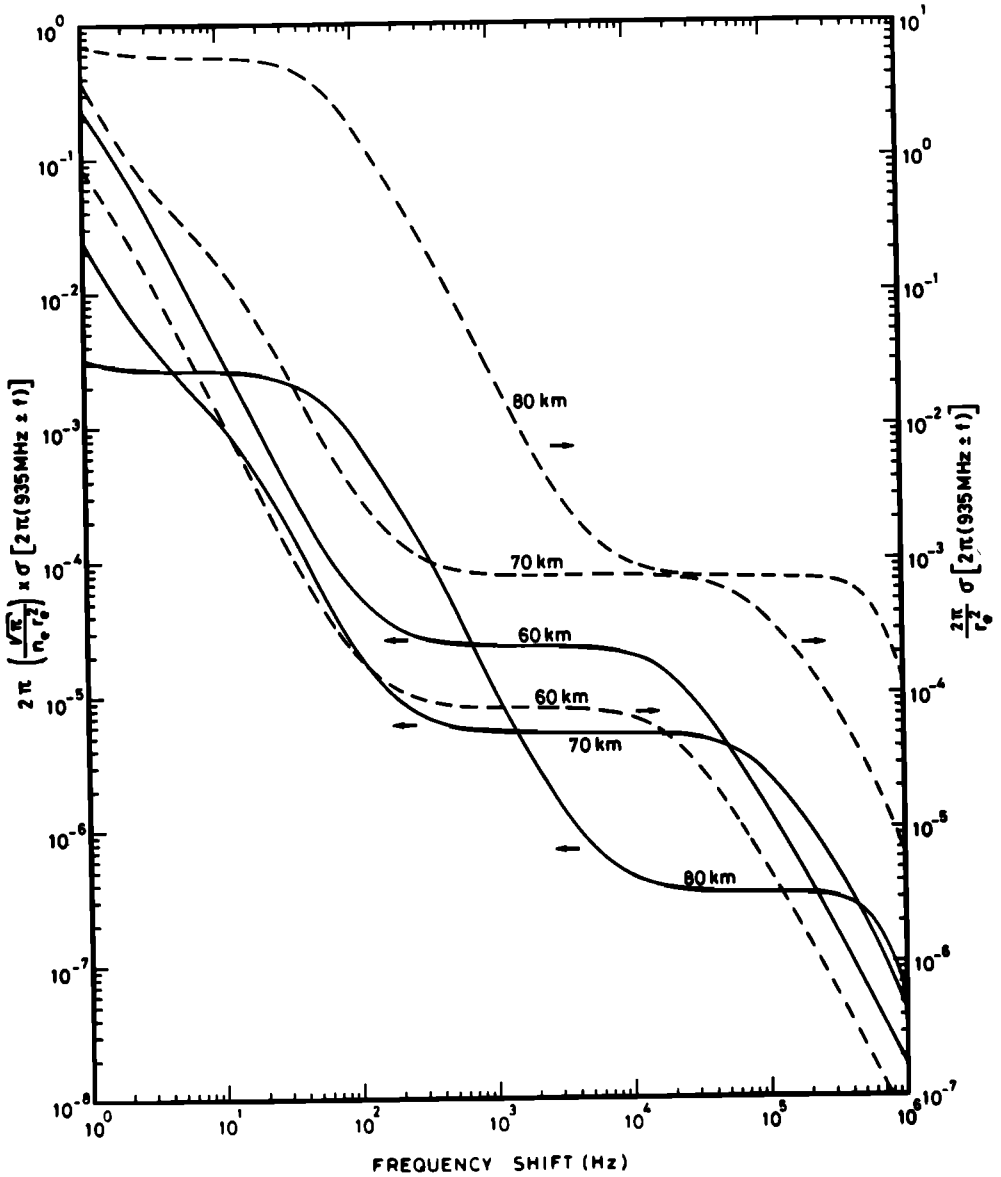

Fig. 1. Incoherent scatter cross sections as a function of frequency shift for an incident frequency of 935 MHz. Solid curves correspond to normalized cross sections (left-hand scale). Dashed curves (right-hand scale) correspond to cross sections expressed in terms of the classical electron radius r_e. Calculations are made for three altitudes with the equivalent ionospheric model deduced from detailed computations of *Wisemberg and Kockarts* [1980].

σ_C is simply given by

$$\sigma_C = \frac{n_e r_e^2}{\pi} \frac{L_e}{\omega^2 + (L_e + L_-)^2} \tag{34}$$

This approximation is also valid at zero-frequency shift, as can be seen on Figure 3 where the total cross section at $f = 0$ is shown as a function of height. The solid curve corresponds to results obtained with our detailed formulation; σ_{MFK} corresponds to the results given by Mathews and Fukuyama and Kofman. When negative ions are completely ignored, one obtains curve labeled σ_+. The dotted-dashed curve σ_C is obtained with (34) for $\omega = 0$. It appears that our approximation for chemical fluctuation fits the detailed calculation below 75-km altitude, where negative ions become important. The frequency shift dependence given by the approximation (34) is able to reproduce the spectra of Figure 2 as long as chemical fluctuations are important. Therefore a measured spectrum with high resolution in frequency shift should give immediately an accurate value of $\lambda = L_e/L_-$, since the effective loss rates are directly proportional to the width of the ionic component.

The total scattered power P_{MFK} per unit volume has been derived by *Mathews* [1978] and by *Fukuyama and Kofman* [1980] in the absence of chemical fluctuations. Furthermore, *Fukuyama and Kofman* [1980] also deduced an approximate expression P_{iMFK} for the ion component. Since the chemical part σ_C given by (34) is easily integrable, we approximate the present total power P_T by

$$P_T = P_{iC} + P_{MFK} \tag{35}$$

with

$$P_{iC} = n_e L_e/(L_e + L_-) \tag{36}$$

This total power is shown as a function of height in Figure 4,

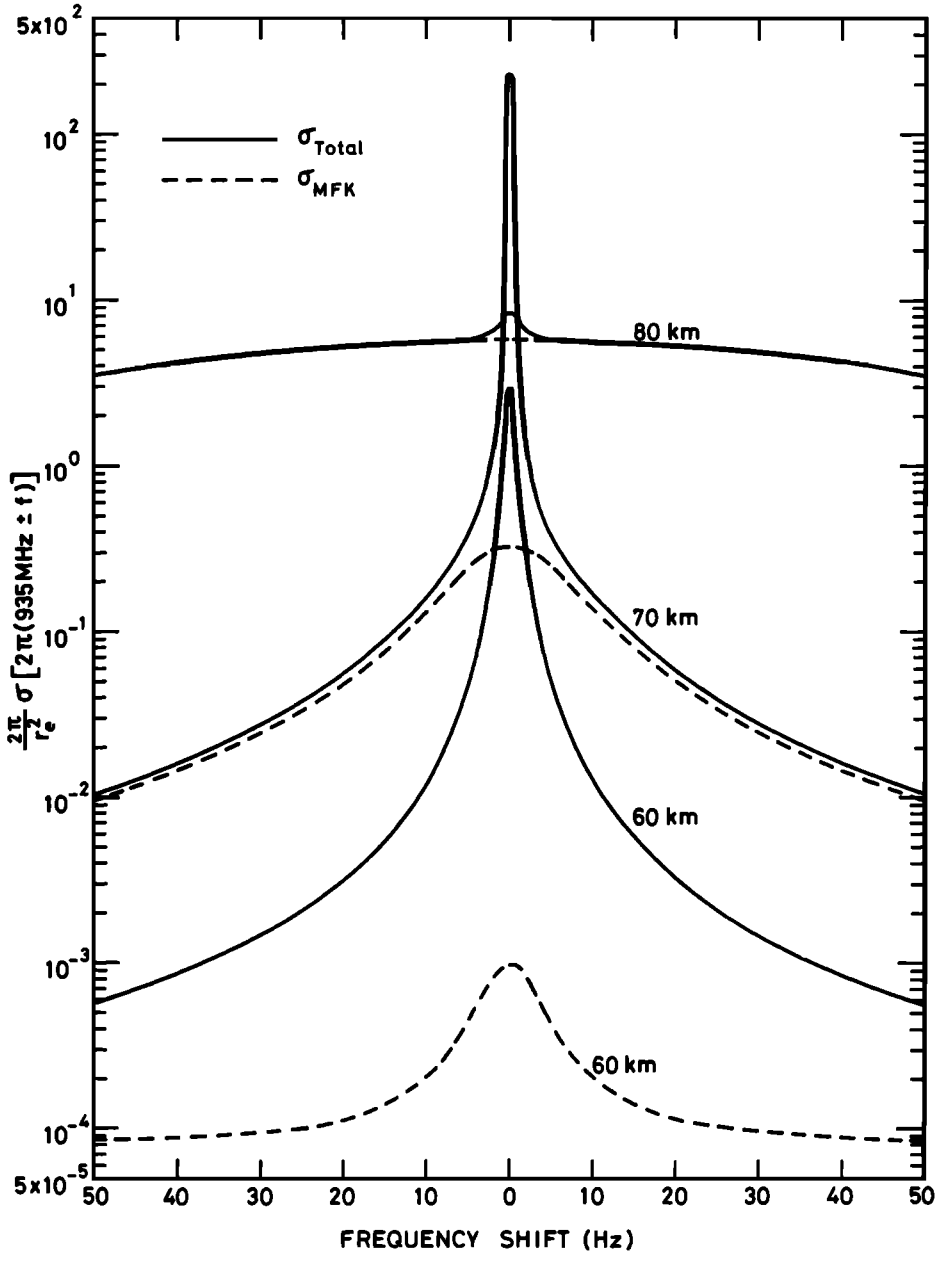

Fig. 2. Incoherent scatter cross sections at 60-, 70-, and 80-km altitude as a function of frequency shift. Solid curves correspond to present results (σ_{total}), and dashed curves (σ_{MKF}) are obtained from expressions given by *Mathews* [1978] and by *Fukuyama and Kofman* [1980].

where P_{MFK} is given for comparison. When chemical fluctuations are neglected, ionic powers with and without negative ions are indicated by P_{iMFK} and P_{i+}, respectively. The chemical part P_{iC} becomes almost identical to P_{MFK} below 65 km in the present ionospheric model. Below this altitude the total power is approximately a factor of 2 higher than the value obtained without chemical fluctuations. It appears again that chemical fluctuations play a significant role in the height range where λ becomes comparable to or greater than 1.

5. CONCLUSION

The continuum theory of incoherent backscattering is extended to include possible effects of production and loss terms in the continuity equations. Chemical reactions can be considered as probabilistic processes which induce additional fluctuations of the particle concentrations. Such fluctuations are superimposed to the classical thermal fluctuation which results from collisions between particles without any change of the identity of the particles. When production and loss terms are considered in the lower D region, it appears that the switching reactions between negative ions and electrons are sufficiently fast to induce a fluctuation of the electron concentration which is capable of modifying the classical incoherent scatter spectrum based on pure thermal fluctuations. The ion component of the backscattering cross section is strongly enhanced for frequency shifts below 20 Hz at altitudes where the ratio λ between negative ions and electrons is greater than 1. As a consequence, high-resolution measuremens should pro-

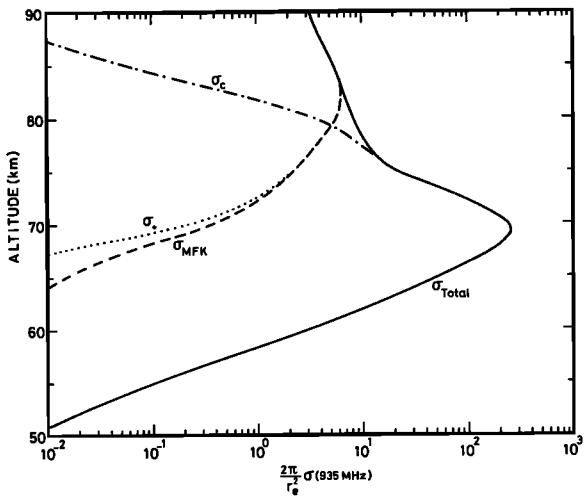

Fig. 3. Vertical distribution of incoherent scatter cross section for zero frequency shift; α_{total} and σ_{MKF} have same meaning as in Figure 2; σ_+ is obtained in the absence of negative ions, and σ_C represents chemical fluctuations approximated given by (34).

vide a direct determination of the ratio λ, since the shape, width, and amplitude of the backscattering spectra influenced by chemical fluctuations essentially depend on the electron and negative ion loss rates L_e and L_-. These two quantities allow a direct determination of λ with (15) which is very accurate over the height range where negative ions play a significant role in the lower D region. Furthermore, the total power of the incoherent scatter spectra is increased by a factor of 2 below 70-km altitude for the ionospheric model adopted in the present calculations. The ionic power is, however, increased by a much larger factor, which may reach 2 orders of magnitude at 65 km. These facts should make the experimental detection easier when sufficient frequency resolution is available.

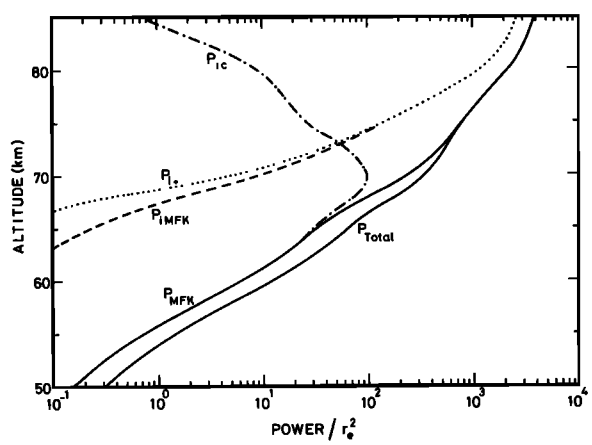

Fig. 4. Vertical distribution of total power P_{total}. Results of *Mathews* [1978] and *Fukuyama and Kofman* [1980] are indicated by solid curve P_{MFK}. The corresponding ion component is labeled P_{iMFK}, whereas P_{i+} gives the contribution of positive ions. Effect of chemical fluctuations is represented by curve P_{iC}, which becomes identical to the total power P_{MFK} below 65-km altitude.

APPENDIX: MATRIX EXPRESSIONS

The equivalent ionospheric model described in section 2 leads to the following one-dimensional continuity equations:

$$\frac{\partial n_e}{\partial t} + \frac{\partial}{\partial z}(n_e u_e) = \gamma_e + n_- L_- - n_e L_e - n_e n_+ \alpha_e \quad \text{(A1)}$$

$$\frac{\partial n_-}{\partial t} + \frac{\partial}{\partial z}(n_- u_-) = n_e L_e - n_- L_- - n_- n_+ \alpha_- \quad \text{(A2)}$$

$$\frac{\partial n_+}{\partial t} + \frac{\partial}{\partial z}(n_+ u_+) = \gamma_e - n_+ n_e \alpha_e - n_+ n_- \alpha_- \quad \text{(A3)}$$

where the various production and loss terms are obtained from (1) to (5) in section 2. Concentrations n_s are assumed to have a steady state component n_{s0} and a fluctuating component n_s' proportional to exp $[i(\omega t - kz)]$. The continuous component of u_s is assumed to be zero, but the fluctuating part is also proportional to exp $[i(\omega t - kz)]$ [*Tanenbaum*, 1968]. Substituting n_s and u_s by their expressions in (A1) to (A3) and neglecting second-order fluctuations, one obtains the matrix equation (20), where **A** is given by

$$\mathbf{A} = \omega^{-1} \cdot \begin{bmatrix} \omega - i(L_e + \alpha_e n_{+0}) & iL_-\lambda & -i\alpha_e n_{+0} \\ iL_e/\lambda & \omega - i(L_- + \alpha_- n_{+0}) & -i\alpha_- n_{+0} \\ -i\alpha_e n_{e0} & -i\alpha_- n_{+0} & \omega - i(\alpha_e n_{e0} + \alpha_- n_{-0}) \end{bmatrix} \quad \text{(A4)}$$

with $\lambda = n_{-0}/n_{e0}$. It has been shown in section 2 that all losses resulting from recombination processes are negligible compared to the effective loss rates L_e or L_-. Although matrix **A**, can be used in its form (A4), it is easier to adopt the approximate expression

$$\mathbf{A} = \omega^{-1} \begin{bmatrix} \omega - iL_e & iL_e & 0 \\ iL_- & \omega - iL_- & 0 \\ 0 & 0 & \omega \end{bmatrix} \quad \text{(A5)}$$

where λ has been replaced by (15).

In the linearized energy equation (21), **Q** and **R** are diagonal matrices whose elements are given by

$$Q_{(s,s)} = (5/3)m_s V_s^2/(i\omega + \sigma_s) \quad \text{(A6)}$$

and

$$R_{(s,s)} = (3/5)\sigma_s Q_{(s,s)} \quad \text{(A7)}$$

with $V_s^2 = KT_{s0}/m_s$ and $\sigma_s = 2m_s\nu_{sn}/(m_s + m_n) + (5/2)k^2V_s^2/(c_s\nu_{sn})$ when the thermal conductivity λ_s in (21) is taken from *Tanenbaum* [1968], c_s being a numerical constant between 1 and 2.

Maxwell's equation relating the displacement current to the current density is used in the same way as *Tanenbaum* [1968] for expressing the electric field in the momentum equation (18). After linearization one obtains the following matrix equation

$$(\mathbf{G}+\mathbf{J})\begin{bmatrix} u_e' \\ u_-' \\ u_+' \end{bmatrix} + \frac{\omega}{k}\mathbf{V}^{-1}\begin{bmatrix} p_e'/n_{e0} \\ p_-'/n_{-0} \\ p_+'/n_{+0} \end{bmatrix} = \frac{i\omega}{k^2 K T_{e0}}\mathbf{T}\begin{bmatrix} F_e' \\ F_-' \\ F_+' \end{bmatrix} \tag{A8}$$

where G, V, and T are diagonal matrices and J represents the coupling resulting from the electric field. The diagonal elements of V and G are given by

$$V_{(s,s)} = m_s V_s^2 \tag{A9}$$

and

$$G_{(s,s)} = -\omega^2 k^{-2} V_s^{-2} + i\omega[4(3d_s\nu_{sn})^{-1} + \nu_{sn}k^{-2}V_s^{-2}] \tag{A10}$$

where the viscosity η_s in G has been replaced by *Tanenbaum*'s [1968] expression with a numerical constant d_s between 1 and 2. The temperature matrix T is given in terms of nonfluctuating parts T_{s0} by

$$\mathbf{T} = \begin{bmatrix} 1 & 0 & 0 \\ 0 & T_{e0}/T_{-0} & 0 \\ 0 & 0 & T_{e0}/T_{+0} \end{bmatrix} \tag{A11}$$

The electric field coupling matrix for different temperatures of the ionized components is given by

$$\mathbf{J} = \begin{bmatrix} \beta_e^2 & \lambda\beta_e^2 & -(1+\lambda)\beta_e^2 \\ \lambda^{-1}\beta_-^2 & \beta_-^2 & -\lambda^{-1}(1+\lambda)\beta_-^2 \\ -(1+\lambda)^{-1}\beta_-^2 & -\lambda(1+\lambda)^{-1}\beta_+^2 & \beta_+^2 \end{bmatrix} \tag{A12}$$

with $\beta_s = (k\lambda_{sD})^{-1}$. The Debye length for each species is defined by $\lambda_{sD} = [\epsilon_0 K T_{s0}/(n_{s0}e^2)]^{1/2}$, where ϵ_0 is the free space permittivity and e is the electron charge.

When (21) is introduced in the momentum equation (A8), one obtains

$$\mathbf{C}\begin{bmatrix} u_e' \\ u_-' \\ u_+' \end{bmatrix} + \frac{\omega}{k}\mathbf{D}\begin{bmatrix} n_e'/n_{e0} \\ n_-'/n_{-0} \\ n_+'/n_{+0} \end{bmatrix} = \frac{i\omega}{k^2 K T_{e0}}\mathbf{T}\begin{bmatrix} F_e' \\ F_-' \\ F_+' \end{bmatrix} \tag{A13}$$

where $\mathbf{D} = \mathbf{V}^{-1}\mathbf{R}$ is a diagonal matrix whose elements are obtained from (A7) and (A9) such that

$$D_{(s,s)} = \sigma_s/(i\omega + \sigma_s) \tag{A14}$$

Matrix C is a combination of previously defined matrices. Its expression can be written

$$\mathbf{C} = \mathbf{G} + \mathbf{J} + i\omega\mathbf{V}^{-1}\mathbf{Q} \tag{A15}$$

where G is given by (A10), J by (A12), $\mathbf{V}^{-1}$ by the inverse of (A9), and Q by (A6), respectively.

Acknowledgments. The Editor thanks D. T. Farley, J. D. Mathews, and B. S. Tanenbaum for their assistance in evaluating this paper.

REFERENCES

Alcaydé, D., Incoherent scatter data related to thermospheric modelling, *Space Res., 19*, 211–229, 1979.

Banks, P. M., and G. Kockarts, *Aeronomy*, parts A and B, Academic, New York, 1973.

Barakat, R., Theory of the coherency matrix for light of arbitrary spectral bandwith, *J. Opt. Soc. Am., 53*, 317–323, 1963.

Bauer, P., Theory of waves incoherently scattered, *Philos. Trans. R. Soc. London, Ser. A, 280*, 167–191, 1975.

Dougherty, J. P., and D. T. Farley, A theory of incoherent scattering of radio waves by a plasma, *Proc. R. Soc. London, Ser. A, 259*, 79–99, 1960.

Evans, J. V., Theory and practice of ionosphere study by Thomson scatter radar, *Proc. IEEE, 57*, 496–530, 1969.

Fukuyama, K., and W. Kofman, Incoherent scattering of an electromagnetic wave in the mesosphere: A theoretical consideration, *J. Geomagn. Geoelectr., 32*, 67–81, 1980.

Ganguly, S., Incoherent scatter observations of mesopheric dynamics at Arecibo, *Geophys. Res. Lett., 7*, 369–372, 1980.

Ganguly, S., J. D. Mathews, and C. A. Tepley, Thomson scatter radar detection of *D*-region negative ions at Arecibo, *Geophys. Res. Lett., 6*, 89–92, 1979.

Harper, R. M., Preliminary measurements of the ion component of the incoherent scatter spectrum in the 60–90 km region over Arecibo, *Geophys. Res. Lett., 5*, 784–786, 1978.

Harper, R. M., and W. E. Gordon, A review of radar studies of the middle atmosphere, *Radio Sci., 15*, 195–211, 1980.

Mathews, J. D., The effect of negative ions on collision-dominated Thomson scattering, *J. Geophys. Res., 83*, 505–512, 1978.

Seasholtz, R. G., Effect of collisions on Thomson scattering in a magnetic field with unequal electron and ion temperature and electron drift, *J. Geophys. Res., 76*, 1793–1802, 1971.

Seasholtz, R. G., and B. S. Tanenbaum, Effect of collisions on Thomson scattering with unequal electron and ion temperatures, *J. Geophys. Res., 74*, 2271–2275, 1969.

Schunk, R. W., Transport equations for aeronomy, *Planet. Space Sci., 23*, 437–483, 1975.

Schunk, R. W., Mathematical structure of transport equations for multispecies flows, *Rev. Geophys. Space Phys., 15*, 429–445, 1977.

Tanenbaum, B. S., Continuum theory of Thomson scattering, *Phys. Rev., 171*, 215–221, 1968.

Walker, J. C. G., Radar measurement of the upper atmosphere, *Science, 206*, 180–189, 1979.

Wisemberg, J., and G. Kockarts, Negative ion chemistry in the terrestrial *D*-region and signal flow graph theory, *J. Geophys Res., 85*, 4642–4652, 1980.

(Received December 30, 1980;
revised March 20, 1981;
accepted March 20, 1981.)